



LABORATORI NAZIONALI DI FRASCATI
SIS-Pubblicazioni

LNF-99/005(P)
8 Febbraio 1999

**EFFECTS OF DIFFRACTION AND TARGET FINITE SIZE ON
COHERENT TRANSITION RADIATION SPECTRA IN BUNCH
LENGTH MEASUREMENTS**

M.Castellano¹, A.Cianchi¹, G.Orlandi² and V.A.Verzilov¹

¹⁾ *INFN, Laboratori Nazionali di Frascati, P.O. Box 13, I-00044 Frascati, Italy*

²⁾ *INFN, Sezione di Roma 2 and University of Roma Tor Vergata, Italy*

Abstract

Effects of diffraction and the size of the target on TR in the context of CTR-based bunch length measurements are studied on the basis of Kirchoff diffraction theory. Spectra of TR from the finite-size target for several schemes of measurements are calculated in the far-infrared region showing strong distortion at low frequencies. Influence of the effect on the accuracy of bunch length measurements is estimated.

PACS:41.60.-m;41.85.Ew;41.75.Ht

Submitted to Nucl.Instr. & Meth. Phys. Res A.

1 Introduction

Operating with subpicosecond bunches is crucial to the new generation of e^+e^- colliders and FELs for reaching their final goals, which are respectively high luminosity and high peak current. To obtain this result, much depends on the ability to monitor bunch dimensions on such a small scale.

It is now widely recognized that this can be done by making use of coherent radiation (CR) of different types produced by a bunched beam interacting with material targets or external fields. Coherent transition radiation (CTR) is only one among others, but it is now intensively used due to its simplicity of implementation and the small perturbation produced on the beam. Another example is the coherent diffraction radiation, that is essentially a special case of CTR, but, being nonintercepting, promises to be advantageous for high current and low-emittance machines.

CTR is emitted by a particle bunch crossing the boundary between two media. Coherent emission takes place at wavelengths comparable with, or longer than, the bunch length. In this case all electrons in the bunch produce radiation more or less in phase, and, as a result, a large enhancement in the emitted power is observed with respect to the ordinary incoherent transition radiation (TR) (for details see reviews [1,2] and an exhaustive list of references therein). The power spectrum of CTR from an individual bunch is given by

$$S_{CTR}(\omega) = N^2 F(\omega) S_{TR}(\omega) , \quad (1)$$

where N is the number of electrons in the bunch, S_{TR} is the power spectrum of TR produced by a single particle and $F(\omega)$ is the bunch form-factor connected through the Fourier transform to the spatial charge distribution

$$F(\omega) = \left| \int dz h(z) e^{i(\omega/c)z} \right|^2 , \quad (2)$$

where $h(z)$ is the normalized charge distribution projected on the direction of the beam momentum (coherence effects due to the bunch transverse dimensions are not considered in this paper). The power spectrum is usually obtained either by a direct spectroscopic measurement or by an autocorrelation technique in the time domain. In any case Eqs. (1) and (2) imply that the bunch longitudinal dimension can be extracted from the measured CTR spectrum if the incoherent TR spectrum is known. In practice, however, Eq. (1) must include also a number of experimental factors, functions of frequency, that introduce some difficulties in the bunch length determination. The limited bandwidth of the detector, as well as diffraction effects due to finite apertures in the radiation transport channel, are the

main factors causing losses of the low frequency part of the measured spectrum; this is true for all CR- based beam diagnostics independent of the radiation used.

Recently, the proper role of the size of the target in modulating the power spectrum of incoherent TR was shown [3,4]. It was found that the size of a target used to produce radiation can be a factor defining spectral and angular features of the emitted photons. The effect occurs when the parameter $\gamma\lambda$, where γ is the relativistic factor of the beam and λ is the radiation wavelength, exceeds the transverse dimensions of the target. While for visible light, since λ is small, the effect is expected at very high energies ($\gamma \geq 10^5$), for CTR at $\lambda \approx 1$ mm it is observable already at γ of a few tens. The TR spectrum from a finite target is a complex function of the beam energy, target extensions, frequency and angle of emission, i.e, very different from the flat spectrum given by the Frank formula, that has been used so far. The effect appears always as a suppression of the spectrum at low frequencies and, therefore, it proves to be important for the analysis of bunch length measurements using CTR.

The low frequency spectrum cutoff, independently of the source, leads to a considerable uncertainty in bunch length and shape determination. Particularly, the precise knowledge of the spectrum over a wide range is a necessary requirement for bunch shape reconstruction using the Kramers-Kronig method [7]. The problem is also important for the autocorrelation technique because of the unambiguous relation between frequency and time domains; the complex optics required in this case makes the effect more evident. While the problem of the detector bandwidth can be solved, even in part, by a calibration of the detector efficiency, others must to be computed or modeled in some way.

For these reasons we believe that a theoretical study of the problem in question is of some value for both the design of experiments and data analysis. In the pioneering work [3], the treatment of the problem of the transverse size of the target in CTR experiments was performed for an electron passing through a thin layer of transparent matter using a perturbation technique, while metallic screens are normally used due to their higher reflectivity. Later, the same authors [5] studied the case of a thin absorbing layer and TR emitted in the forward direction. As a consequence, the resulting picture of the effect must include interference between TR, the particle field and diffraction radiation and, therefore, becomes rather complex. Again, a typical geometry for bunch length measurements consists of a target tilted at 45 degrees with respect to the incoming beam, the radiation being detected at 90 degrees.

In this paper we calculate the single particle spectrum emitted in the backward direction from a finite-size target, in the presence of diffraction by the collection optics and the environment. It has been shown [6] that properties of the backward radiation are almost identical to those of radiation emitted at 90 degrees. Since diffraction phenomena

are generally too complicated to be computed in a rigorous way, we restrict our analysis to a number of simplified models, that, nevertheless, cover the majority of experimental situations. A particular emphasis is placed on the problem of the finite size of the target, as less known.

2 Effects of diffraction and target size on TR spectra

In the calculations, we rely on the approach already used in our previous work [9]. The method is, essentially, the application of the Kirchoff diffraction theory to describe the propagation of the field generated by a charged particle on the boundary between the vacuum and a perfect conducting material. TR is considered to emerge in the backward directions with respect to the momentum of the particle crossing the boundary at normal incidence. Three different schemes of measurement, close to those typically encountered in practice, are investigated.

2.1 Spectrum of TR filtered by a finite aperture

The first scheme considered is the simplest for spectroscopic measurements. It is characterized by the presence of only one circular diaphragm between the emitting screen and the detector, typically representing the window separating the vacuum chamber of an accelerator from the detector environment, and no other collecting optics. For ease of calculation we assume a cylindrically symmetric geometry. A circular target with a radius r made of a perfect metal is placed at a distance a from the diaphragm, while b is the distance between the diaphragm and the detector having a diameter $2d$ (Fig. 1a). The incident particle with charge q and velocity v hits the target at the center. Emerging TR propagates in the z direction. Let us introduce three different sets of coordinates $(x_s, y_s), (\xi, \eta)$ and (x, y) for the target, diaphragm and detector planes, respectively.

The TR field components at the arbitrary point P(x,y) in the detector plane in the Fresnel approximation, and neglecting phase constants, are found to be

$$E_{x,y}(P, \omega) = -\frac{k^2}{(2\pi)^2} \frac{1}{ab} \int d\xi d\eta \int dx_s dy_s f_{x,y}(x_s, y_s) \times e^{i(k/2a)[(\xi-x_s)^2+(\eta-y_s)^2]} e^{i(k/2b)[(x-\xi)^2+(y-\eta)^2]} , \quad (3)$$

where the function $f_{x,y}$ is given by

$$f_{x,y}(x_s, y_s) = \frac{iq}{\pi v} \int d\alpha_x d\alpha_y \frac{\alpha_{x,y}}{\alpha^2 + \alpha^2} e^{i(\alpha_x x_s + \alpha_y y_s)} . \quad (4)$$

and represents the TR transverse components on the target plane. In Eqs. (3) and (4) $k = \omega/c$ is the photon wave vector, $\varkappa_{x,y}$ are its projections on the xy plane and $\alpha = \omega/v\gamma$.

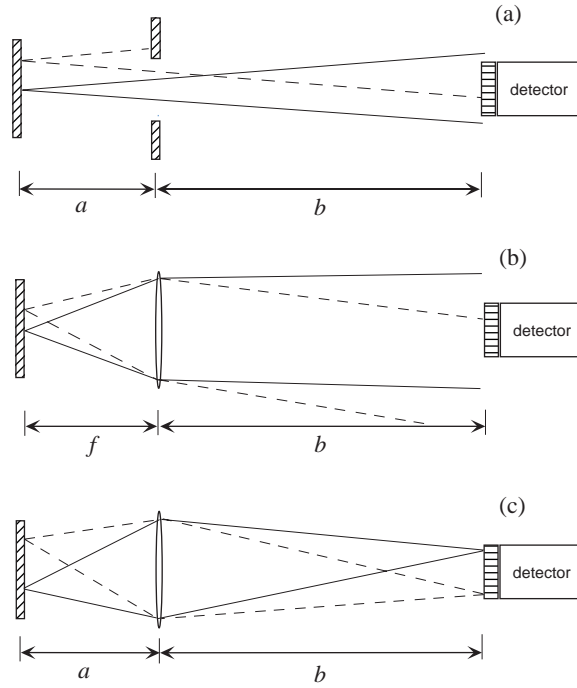


Figure 1: Three schemes of measurements under consideration: a) TR beam emitted by the target is filtered by a diaphragm, b) the target is placed in the front focal plane of a lens having the focus length f , c) the target is imaged onto the detector by the lens.

In cylindrical coordinates we have:

$$\varkappa_{x,y} = \begin{Bmatrix} \varkappa_x \\ \varkappa_y \end{Bmatrix} = \varkappa \begin{Bmatrix} \cos \psi \\ \sin \psi \end{Bmatrix}, \begin{Bmatrix} x_s \\ y_s \end{Bmatrix} = \rho_s \begin{Bmatrix} \cos \varphi \\ \sin \varphi \end{Bmatrix}, \begin{Bmatrix} x \\ y \end{Bmatrix} = \rho \begin{Bmatrix} \cos \chi \\ \sin \chi \end{Bmatrix}. \quad (5)$$

Using these notations, after several simple integrations over the angular variables, and omitting the phase factor containing ρ^2 , we obtain the expression for the field in a general form:

$$E_{x,y}(P, \omega) = \frac{q}{2\pi^2 v} \frac{k^2}{ab} \int d\rho_s \rho_s \int d\varkappa \frac{\varkappa^2 J_1(\varkappa \rho_s)}{\varkappa^2 + \alpha^2} e^{i(k/2am)\rho_s^2} \times \int d\varphi \begin{Bmatrix} \cos \varphi \\ \sin \varphi \end{Bmatrix} e^{-i(k/am)\rho \rho_s \cos(\varphi - \chi)} \mathcal{L}(p), \quad (6)$$

where $m = 1 + b/a$, J_1 is the Bessel function of the first kind and

$$\mathcal{L}(p) = 2\pi e^{i(k/2bm)p^2} \int_0^D d\zeta \zeta e^{i(km/2b)\zeta^2} J_0(k\zeta p/b), \quad (7)$$

$$p = \sqrt{\rho^2 + (b^2/a^2)\rho_s^2 + 2(b/a)\rho \rho_s \cos(\varphi - \chi)}.$$

As follows from Eq. (6), the field in P is built up by a coherent summation of the waves emitted by all points of the source and so it, therefore, depends on both the shape and the size of the target. The phase factor linearly dependent from ρ_s is of Fraunhofer type and, consequently, responsible for fields at far distances from the source, while that containing ρ_s^2 provides a first order Fresnel correction to the Fraunhofer approximation. The function \mathcal{L} , mainly determined by the integral over the diaphragm surface, gives a contribution from the standard diffraction by the aperture.

The above integral is well known (see, e.g., [10]) and is expressed in terms of the Lommel functions:

$$\mathcal{L}(p) = \frac{2\pi ib}{km} \left\{ 1 - e^{i(k/2bm)(p^2+m^2D^2)} [V_0(p) - iV_1(p)] \right\}, \quad (8)$$

where the Lommel functions V_n can be written in our case in the form:

$$V_n(p) = \sum_{l=0}^{\infty} (-1)^l \left(\frac{p}{mD} \right)^{n+2l} J_{n+2l} \left(\frac{kD}{b} p \right). \quad (9)$$

Thus, Eq. (6) includes effects given by both the size of the target and the diffraction produced by the diaphragm. The latter is well known to, basically, produce a low frequency spectrum cutoff, almost entirely defined by the diaphragm aperture and angular acceptance. However, Eq. (6) can be hardly analyzed analytically in its general form. From this point on, we found it reasonable to separate the two effects and focus our study on that of the target size. To this end we formally let D tend to ∞ . So that \mathcal{L} reduces to a constant

$$\mathcal{L}_{\infty} = \frac{2\pi ib}{km}. \quad (10)$$

Practically, the better the inequality $d \gg \sqrt{b\lambda/m}$ is fulfilled, the more the approximation is adequate.

We must then consider the phase factor in Eq. (6) that is quadratic in ρ_s and previously recognized as a Fresnel correction factor. To clarify how it can affect the TR spectrum, we first draw attention to the correspondence of the Fraunhofer approximation to the so called wave zone or radiation zone concept. The wave zone is usually specified as the spatial domain where a spherical wave in the proximity of the observation point can be considered a plane one. In this context, the above phase factor is the first order corrections to the wave zone approximation due to the extended character of the source and the sphericity of wave fronts at the point P. As seen, its effect is essentially to give a limit $\rho_s \leq \sqrt{am\lambda}$ to the size of the area on the source surface that mainly forms the field at P: source points lying outside of this region do not give any noticeable contribution because

of the destructive interference. Obviously, for a finite-size target these corrections can be neglected if

$$r \ll \sqrt{am\lambda}. \quad (11)$$

This condition is well satisfied for long wavelengths, but unavoidably breaks down at short ones and then the correction factor reduces the "effective" size of the target. On the other hand, decreasing the wavelength, the quantity $\lambda\gamma$ decreases faster than $\sqrt{am\lambda}$ and, therefore, at sufficiently small wavelengths, such that

$$\lambda \ll \frac{am}{\gamma^2}, \quad (12)$$

the correction factor does not play any role and the TR spectrum becomes indistinguishable from the conventional spectrum from an infinite target.

The inequality Eq. (12) has a more general form

$$\lambda\gamma^2 \ll z, \quad (13)$$

where z is the distance from the TR source to the observation point. This condition is of great importance for applications of TR, since it establishes the boundary of the wave zone and, therefore, the validity of the standard TR formulae. When condition Eq. (13) is violated, even an infinite target acts like a finite-size one with an "effective" dimension depending on the wavelength and the distance to the observation point.

In the far-infrared region, that represents our main interest, the condition Eq. (11) can be well fulfilled by adjusting the distance between the target and detector. So that, using Eq. (10), Eq.(6) can be significantly simplified, giving

$$E_{x,y}(P, \omega) = -\frac{2q}{v} \frac{k}{am} \left\{ \begin{array}{l} \cos \chi \\ \sin \chi \end{array} \right\} \int d\rho_s \rho_s \int d\kappa \frac{\kappa^2 J_1(\kappa\rho_s)}{\kappa^2 + \alpha^2} J_1\left(\frac{k\rho}{am}\rho_s\right). \quad (14)$$

The upper integration limit with respect to κ represents a delicate problem. In fact, TR appears as a result of a "reflection" by the target of the pseudophotons arising when the fast particle electromagnetic (EM) field is expanded as an infinite set of plane waves (Weizsäcker- Williams representation). This implies that in a rigorous theory κ must run the full range from 0 to ∞ . But actually, pseudophotons with $\kappa > k$ cannot transform into real ones and propagate in a free space. Since, in this paper, fields are considered at large (compared to the wavelength) distances from the target, it is a reasonable assumption to regard κ as being confined within a range between 0 and k . For $\gamma \gg 1$ the truncated integral has the rather accurate approximate value

$$\int_0^k d\kappa \frac{\kappa^2 J_1(\kappa\rho_s)}{\kappa^2 + \alpha^2} \simeq \alpha K_1(\alpha\rho_s) - \frac{J_0(k\rho_s)}{\rho_s}, \quad (15)$$

where K_1 is the modified Bessel function of the first kind. A simple analysis of Eq.(15) reveals that the second term in the right-hand side is of importance mainly in the region $\rho_s \leq \lambda$, where it compensates the irregular behaviour of the first term as $\rho \rightarrow 0$, while beyond this region it provides only a decaying modulation of the first term. Since the next step in the calculation is integrating over ρ_s , for $\lambda \ll r$ we expect a small contribution from the second term compared to the first one. However, for wavelengths comparable or larger than r it has to be taken into account. This gives

$$\int_0^r d\rho_s \rho_s \left[\alpha K_1(\alpha \rho_s) - \frac{J_0(k \rho_s)}{\rho_s} \right] J_1(\delta \rho_s) = \Phi(r, \alpha, k, \delta), \quad (16)$$

where δ stands for $k\rho/am$ and

$$\begin{aligned} \Phi(r, \alpha, k, \delta) = & \frac{\delta}{\alpha^2 + \delta^2} - \frac{\alpha r}{\alpha^2 + \delta^2} [\delta K_1(\alpha r) J_0(\delta r) + \alpha J_1(\delta r) K_0(\alpha r)] \\ & - \int_0^r d\rho_s J_0(k \rho_s) J_1(\delta \rho_s). \end{aligned} \quad (17)$$

Substituting Eq. (16) into Eq. (14), we obtain

$$E_{x,y}(P, \omega) = -\frac{2q}{v} \frac{k}{am} \left\{ \begin{array}{l} \cos \chi \\ \sin \chi \end{array} \right\} \Phi(r, \alpha, k, \delta). \quad (18)$$

Eq. (18) gives the TR field from a finite-size target in the wave zone. It is interesting to note the connection with diffraction radiation (DR): in Eq. (17) the second and third terms represent exactly the DR from a circular hole of a radius r in an infinite screen, while the first one gives the conventional TR. Thus, TR from a finite-size target appears as the difference between the ordinary TR and DR in accordance with the Babinet's principle.

The differential power spectrum is given by

$$S_{\omega,P}(\rho) = \frac{q^2}{\pi^2 c} \frac{k^2}{\beta^2 a^2 m^2} \Phi^2(r, \alpha, k, \delta). \quad (19)$$

The total spectrum registered by the detector is found by integrating Eq. (19) over the detector aperture

$$S_\omega = 2\pi \int_0^d d\rho \rho S_{\omega,P}(\rho). \quad (20)$$

If in this integral one makes the substitution $\rho = am \sin \theta$ and uses θ as the new integration variable, one finally obtains

$$S_\omega = \frac{2q^2}{\pi c} \frac{k^2}{\beta^2} \int_0^{\theta_m} d\theta \sin \theta \cos \theta \Phi^2(r, \alpha, k, k \sin \theta), \quad (21)$$

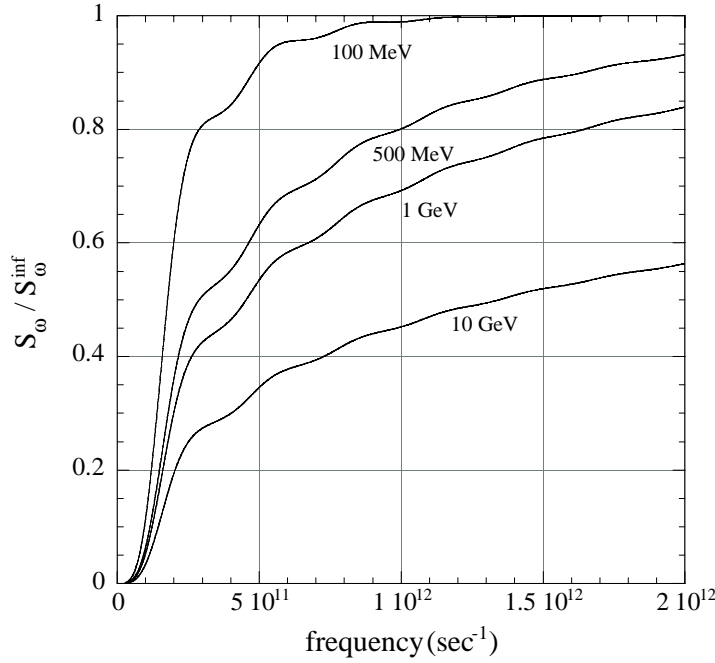


Figure 2: Spectra S_ω of TR in the first scheme of measurements, for a target with radius of 20 mm and a detector angular acceptance of 0.05 rad. Spectra, normalized to the corresponding ones from the infinite target, S_ω^{inf} , are plotted for several beam energies.

where $\theta_m = \arcsin(d/am)$ is the angular acceptance of the detector.

Figures 2 and 3 show the spectra calculated by using Eq. (21) for parameters and frequency ranges typical of bunch length measurements, and normalized to the corresponding spectra from an infinite target. Figure 2 shows spectra for different beam energies. It can be seen that the distortion of the spectrum increases at large energies. This can be simply explained by the fact that the particle field, which scales like $\gamma\lambda$ in the transverse directions, becomes increasingly larger than the target dimension with increasing energies so that its outermost portion, carrying the low-frequency spectral components, contributes less and less to TR. From the condition $\gamma\lambda \geq r$ ($\omega \leq c\gamma/r$) that gives the spectral region influenced by the effect, it follows that this domain expands towards higher frequencies linearly with γ . Spectra for different detector angular apertures are given in Fig. 3. One can see that the suppression effect becomes more pronounced with decreasing angular aperture. This implies that the spectral content of the radiation is no longer constant as in the case of ordinary TR but is a function of the emission angle. The reason for such a kind of correlation can be again understood in terms of the simple picture given above, because the TR at small angles is mostly formed by the periphery of the particle field.

A simple formula for the spectral-angular distribution can be obtained from Eqs. (19) and (17) in the special case of a high-energy limit such that $\alpha r \ll 1$. Neglecting the in-

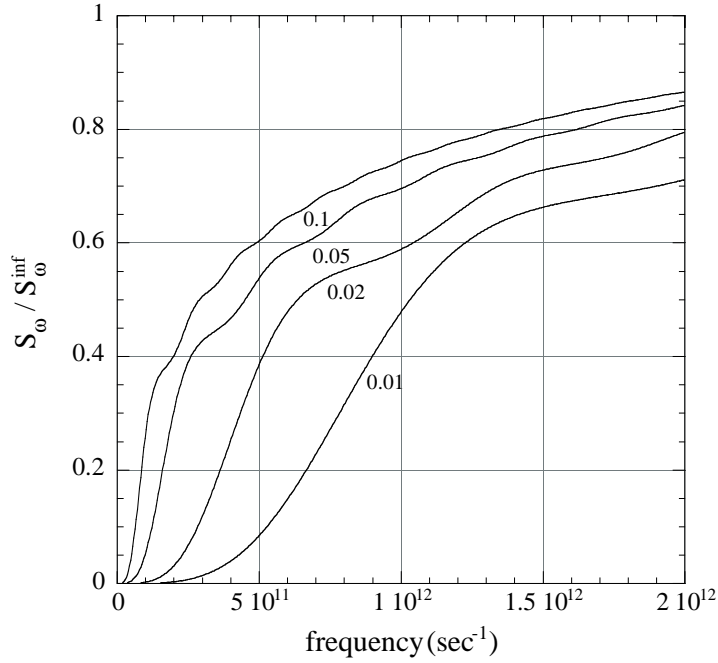


Figure 3: Spectra of TR S_ω in the first scheme of measurements for a target radius of 20 mm and beam energy of 1 GeV. Spectra are normalized to the corresponding spectra S_ω^{inf} from the infinite target. Numbers next to the curves are detector angular acceptances in radians.

tegral term in Eq. (17) and defining the angular variable θ as before, we arrive at the formula, that was earlier derived in [4]:

$$S_{\omega,\theta} = S_{\omega,\theta}^{inf} [1 - J_0(kr \sin \theta)]^2, \quad (22)$$

where $S_{\omega,\theta}^{inf}$ is the spectral- angular distribution of the ordinary TR from an infinite target, given by

$$S_{\omega,\theta}^{inf} = \frac{q^2}{\pi^2 c} \frac{\sin^2 \theta}{(1 - \beta^2 \cos^2 \theta)^2}. \quad (23)$$

It follows from Eq. (22) that in contrast to the ordinary TR, that peaks at γ^{-1} , the angular distribution of TR from a finite-size target has the maximum at the larger angle, depending on the wavelength :

$$\theta_{max} \approx \frac{2.8}{kr}. \quad (24)$$

2.2 Spectrum of TR from a target in the focal plane of a lens

The second scheme under consideration (Fig. 1b) is a simplified geometry normally used in autocorrelation interferometric measurements, when the target is placed in the front fo-

cal plane of a converging lens to produce, behind the lens, a quasi-parallel photon beam. Let us consider a thin lens with diameter $2D$ and focal length f . It is known that the lens introduces a phase advance that is a function of the coordinates on its surface. In the Fresnel approximation, the field in the detector plane can then be obtained by multiplication of Eq. (3) by the phase factor

$$h(\xi, \eta) = e^{-i(k/2f)(\xi^2 + \eta^2)} . \quad (25)$$

By the same computation as in the case of the previous scheme we arrive at the formula, analogous to Eq. (6),

$$\begin{aligned} E_{x,y}(P, \omega) &= \frac{q}{2\pi^2 v} \frac{k^2}{fb} \int d\rho_s \rho_s \int d\chi \frac{\chi^2 J_1(\chi \rho_s)}{\chi^2 + \alpha^2} e^{i(k/2f)\rho_s^2(1-b/f)} \\ &\times \int d\varphi \begin{Bmatrix} \cos \varphi \\ \sin \varphi \end{Bmatrix} e^{-i(k/f)\rho \rho_s \cos(\varphi - \chi)} \mathcal{L}(p) . \end{aligned} \quad (26)$$

As before \mathcal{L} is expressed through the Lommel function

$$\begin{aligned} \mathcal{L}(p) &= \frac{2\pi i b}{k} [1 - e^{i(k/2b)(p^2 + D^2)} [V_0(p) - iV_1(p)]] , \\ V_n(p) &= \sum_{l=0}^{\infty} (-1)^l \left(\frac{p}{D}\right)^{n+2l} J_{n+2l} \left(\frac{kD}{b} p\right) , \\ p &= \sqrt{\rho^2 + (b^2/f^2)\rho_s^2 + 2(b/f)\rho \rho_s \cos(\varphi - \chi)} . \end{aligned} \quad (27)$$

In contrast to the previous scheme, the Fresnel correction factor in Eq. (26) can be set exactly to 1 by choosing $b = f$, i.e., by placing the detector in the back focal plane of the lens. Apart from this, Eqs. (26) and (27) are identical to the corresponding Eqs. (6)-(9) if one puts in the latter $a = f$ and $m = 1$. The power spectrum, in the infinite lens approximation, is thus given by Eq. (21) with

$$\theta_m = \arcsin(d/f) . \quad (28)$$

The similarity between the first and second scheme can be seen by simple ray tracing: the effect of the lens is basically to "draw" the detector towards the target, resulting in an increase of the angular acceptance of the system.

2.3 Spectrum of TR in the target image plane

Here the diaphragm of the first scheme is replaced by a lens of the same size and a and b are chosen such that the condition $1/a + 1/b = 1/f$ is satisfied (Fig. 1c). In this geometry

the target is simply imaged onto the detector. The expression for the field is obtained from Eq. (3) and Eq. (25)

$$E_{x,y}(P, \omega) = \frac{q}{2\pi^2 v} \frac{k^2}{ab} \int d\rho_s \rho_s \int d\chi \frac{\chi^2 J_1(\chi \rho_s)}{\chi^2 + \alpha^2} e^{i(k/2a)\rho_s^2} \times \int d\varphi \begin{Bmatrix} \cos \varphi \\ \sin \varphi \end{Bmatrix} \mathcal{L}(p), \quad (29)$$

where, as before, \mathcal{L} is the pattern resulting from the diffraction on the lens, that in this case is given by the well-known expression

$$\mathcal{L}(p) = \frac{2\pi a D}{kp} J_1\left(\frac{kD}{a}p\right), \quad (30)$$

$$p = \sqrt{\varrho^2 + \rho_s^2 + 2\varrho\rho_s \cos(\varphi - \chi)},$$

with $\varrho = \rho/M$, where $M = b/a$ is the lens magnification. There is a principle difference between this scheme and the previous ones. In fact, in the first and second models all the points of the target contribute to the field at any particular point in the detector plane, while, in the present case every point in the detector plane is an image (diffraction limited for a finite-size lens) of the corresponding point of the target. This fact is responsible for the disappearing in Eq. (29) of the phase factor linear in ρ_s .

As a consequence of the simple form of the function \mathcal{L} , Eq. (29) can be shown [9] to reduce to

$$E_{x,y}(P, \omega) = \frac{q}{\pi v} \frac{1}{M} \begin{Bmatrix} \cos \chi \\ \sin \chi \end{Bmatrix} \int d\chi \frac{\chi^2}{\chi^2 + \alpha^2} \times \sum_{l=1}^{\infty} R_l \frac{J_{2l}(\delta \varrho)}{\varrho} \int d\rho_s e^{i(k/2a)\rho_s^2} J_1(\chi \rho_s) J_{2l}(\delta \rho_s). \quad (31)$$

The spectrum of radiation can be calculated analytically for the infinite lens and neglecting the Fresnel correction phase factor, as before. Using the fact that the infinite lens establishes an unambiguous correspondence between the source and image planes, one gets

$$\mathcal{L}_{\infty} = \begin{cases} (2\pi)^2 \frac{a^2}{k^2} \frac{\delta(\rho_s - \varrho)}{\rho_s} \delta(\varphi - \chi - \pi) & , \varrho \leq r \\ 0 & , \varrho > r \end{cases}. \quad (32)$$

After integrating over the target area, Eq. (29) becomes

$$E_{x,y}(P, \omega) = -\frac{2q}{v} \frac{1}{M} \begin{Bmatrix} \cos \chi \\ \sin \chi \end{Bmatrix} \int d\chi \frac{\chi^2 J_1(\chi \varrho)}{\chi^2 + \alpha^2}. \quad (33)$$

By making use of Eq. (15), the power spectrum integrated over the detector area is given by

$$S_\omega = \frac{2q^2}{\pi c} \frac{1}{\beta^2} \int_0^{d/M} d\rho \left[\alpha K_1(\alpha\rho) - \frac{J_0(k\rho)}{\rho} \right]^2. \quad (34)$$

In Eq. (34) we imply that $d/M \leq r$, while generally one should integrate from 0 to $\min\{d/M, r\}$.

In contrast to the first and second scheme, where the second term provides just a small corrections at long wavelengths, here it is of great importance to avoid singularities in S_ω . Both terms in Eq. (34) show a divergence at $\rho = 0$, but their difference is finite. This requires special care in a numerical evaluation of the integral, but a divergence-free expression can be obtained by calculating the integral with a finite value for the lower limit of integration and then performing the limit to zero. This gives

$$\begin{aligned} S_\omega = & \frac{2q^2}{\pi c} \frac{1}{\beta^2} \left\{ C - \ln 2 - \frac{1}{2} - \alpha d \left[K_0(\alpha d) K_1(\alpha d) + \frac{\alpha d}{2} [K_0^2(\alpha d) \right. \right. \\ & \left. \left. - K_1^2(\alpha d)] \right] + 2K_0(\alpha d) J_0(kd) + 2k \int_0^d d\rho K_0(\alpha\rho) J_0(k\rho) \right. \\ & \left. + \ln(\alpha d) - \frac{k^2 d^2}{4} {}_3F_4(1, 1, \frac{3}{2}; 2, 2, 2, 2; -k^2 d^2) \right\}, \quad (35) \end{aligned}$$

where $C = 0.5772\dots$ is the Euler's constant and ${}_3F_4$ is the hypergeometric function.

We want to attract attention to the identical role of the target and detector dimensions in affecting the spectrum. In fact, since the intensity distribution in the image plane is just a "magnified" image of that in the source plane, both target and detector are equivalent in producing restrictions on the transverse region over which the power spectrum must be calculated; namely, the spectrum is only determined by the minimum values of d/M and r . Two implications follow immediately. Firstly, the effect of the detector size is of the same nature as that of the target. In particular, the spectrum produced by an infinite target but registered by a finite-size detector is absolutely identical to the spectrum produced from a target of the same size (assuming $M = 1$), provided that it is seen by a detector of large enough dimensions. Secondly, with increasing d , the spectrum given by Eq. (35) must approach that for an infinite target. Actually, as $d \rightarrow \infty$, the whole expression in curly brackets tends to $\ln(\beta\gamma) - \frac{1}{2}$ and Eq. (35) gives the exact result as $v \rightarrow 1$.

The radiation spectra given by Eq. (35) for different beam energies are plotted in Fig. 4.

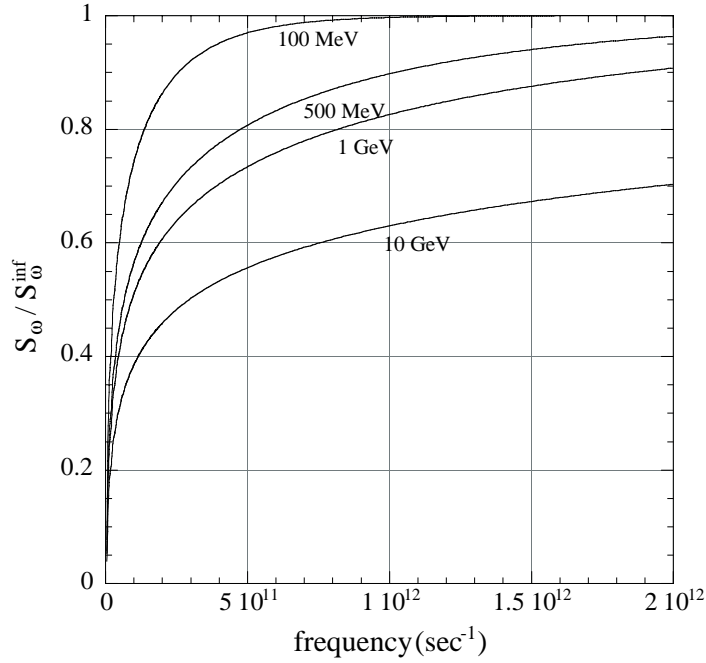


Figure 4: Spectra S_ω of TR in the third scheme of measurements for a target with radius $r=20$ mm (provided that $d/M \leq r$, where d is the detector diameter and M is the lens magnification). Spectra are normalized to the corresponding spectra S_ω^{inf} from the infinite target and given for several beam energies.

3 Uncertainty in CTR bunch length measurements due to the size of the target

In the ideal case, i.e, in the absence of the low frequency suppression, the spectrum of CTR is directly proportional to the bunch form-factor. Therefore, applying an inverse Fourier transform to Eq. (2) an unambiguous determination of the symmetrical component of the charge distribution in the bunch can be performed. Unfortunately, in a real experiment a distortion of the spectrum at low frequencies is always present. The usual practice then consists in empirically selecting part of the spectrum that is assumed unperturbed and recovering from that the bunch length information by assuming the bunch charge distribution shape is known. However, such a procedure can lead to large systematic errors because the selected portion of the spectrum may still be distorted or represents only a very small fraction of the whole spectrum. To solve this problem, it was suggested in [8], and successfully applied to autocorrelation measurements, to add an analytical filter function simulating the frequency cutoff to the expected spectrum and use it to fit the experimental autocorrelation data. Even if very successful in particular cases, the method is difficult to apply to non-Gaussian beams and, besides, the choice of the fitting function is always somewhat arbitrary.

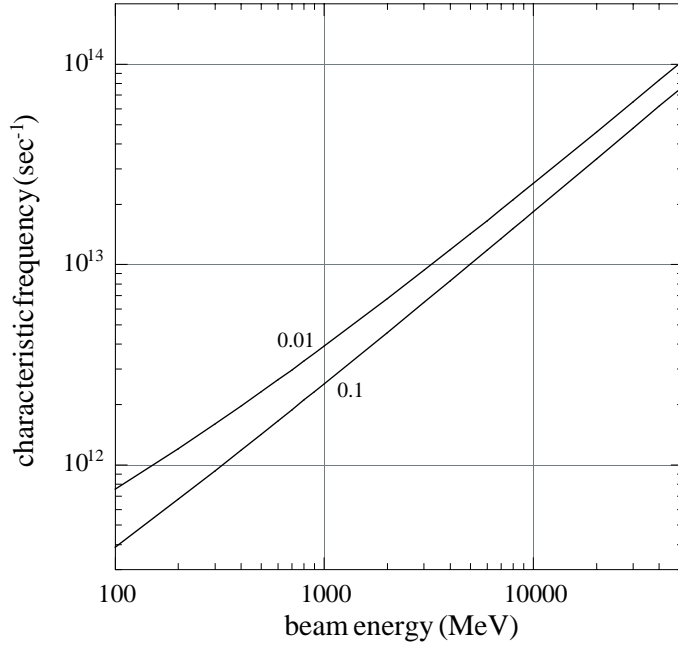


Figure 5: The characteristic frequency ω_{ch} corresponding to a 10% dropoff ($R = 0.9$, where $R = S_\omega/S_\omega^{inf}$) from the high-frequency plateau ($R = 1$) of spectra, for a target radius of 20mm, in the first and second schemes of measurements. Numbers next to the curves are detector angular acceptances in radians.

As stated in the introduction, there are many possible sources for a low frequency suppression of the CTR spectrum, and it is evident that the capability of evaluating quantitatively this effect for at least some of the sources and making the necessary corrections to the experimental spectrum would seriously improve the accuracy of the data analysis. The effects of diffraction in the whole system is usually difficult to calculate, unless there is a single element that defines entirely all properties of the optics. On the other hand, the computations for the finite-size target can be easily performed, using the formulae given in this paper. The corrections for this effect can be important because for sufficiently high beam energies a great portion of the spectrum is modified compared to that of an infinite target. In general, obviously, the usefulness of this correction should be evaluated in relation to the given bunch length and the presence of other possible suppression mechanisms. To this end it is important to characterize the finite-size effect on the frequency scale and give simple rules allowing to estimate, even roughly, the role of the effect in the every particular situation.

As usual for such kind of problems, we define a characteristic frequency ω_{ch} corresponding to a 10% dropoff of spectra from the high-frequency plateau, thus defining the region $\omega > \omega_{ch}$ where the distortion is small. In Fig. 5 and 6 the characteristic fre-

quency ω_{ch} is plotted versus the beam energy for the first two and the third schemes of measurements, respectively.

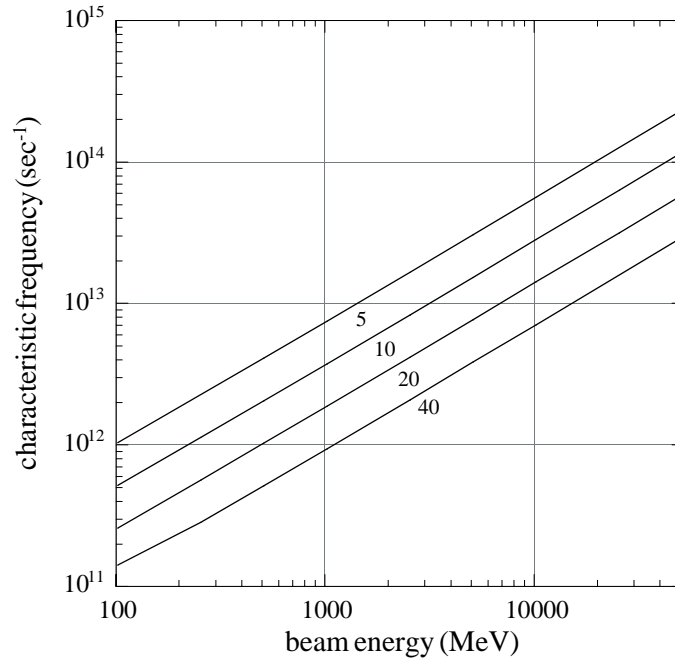


Figure 6: The characteristic frequency ω_{ch} corresponding to a 10% dropoff ($R = 0.9$, where $R = S_\omega/S_\omega^{inf}$) from the high-frequency plateau ($R = 1$) of spectra, for a target radius r in the third scheme. Numbers next to the curves are minimum value of d/M and r in mm, where $2d$ is the detector diameter and M is the lens magnification.

To establish a relation between the characteristic frequency and the bunch length we assume a gaussian bunch shape. The form-factor for the gaussian beam is

$$F(\omega) = e^{-\omega^2/2\sigma_\omega^2}, \quad (36)$$

where σ_ω relates to the bunch length σ_z as $\sigma_\omega = c/\sqrt{2}\sigma_z$. To have a reliable bunch length determination by means of a the Gaussian fit to the spectrum, the latter must be weakly distorted at least in the region $\omega \geq \sigma_\omega$. One may guarantee in this case that the systematic error will be well within 10% if the following condition is satisfied

$$\sigma_z < \frac{c}{\sqrt{2}\omega_{ch}}. \quad (37)$$

Thereby, even qualitatively, the criterion Eq. (37) can be used to estimate in a simple way whether for a given bunch length the effect of the target size is important.

The characteristic frequency can also serve as a parameter allowing to compare the finite-size effect with other sources of low frequency suppression . For the sake of

convenience and ease of evaluation we give here simple approximate relations for ω_{ch}

$$\omega_{ch}(sec^{-1}) = \frac{3.3 \cdot 10^9}{\sqrt[4]{\theta_m(rad)}} E^{0.87}(MeV) \quad (38)$$

and

$$\omega_{ch}(sec^{-1}) = \frac{8.3 \cdot 10^{10}}{d(mm)} E^{0.87}(MeV) \quad (39)$$

found by analyzing the curves of Fig. 5 and 6, respectively.

4 Conclusion

The development of ever shorter electron bunches for x-ray FELs and high energy Linear Colliders makes the measurements of bunch length based on CTR more interesting. For this reason it is important to understand all the sources that can modify the radiation spectrum with respect to the classical "flat" distribution given by the Frank formula. Diffraction from the limited angular acceptance of the experimental apparatus and the finite dimension of the source target are among the main causes of the reduction of the radiation intensity at low frequencies, and have been only slightly considered up to now.

In this paper we have derived rather accurate analytical expressions, with main emphasis on the finite-size target effect, that can help in correcting the experimental results, together with empirical rules that can indicate the need of such a correction, on the basis of the Kirchoff diffraction theory.

The analysis has been performed for some simplified experimental schemes that are most used in practice. As was expected, the effect of the target dimension arises when the target is smaller than the parameter $\gamma\lambda$ that characterizes the transverse extension of the particle EM field. It is important to note that when the radiation detection is performed at a distance $z \leq \lambda\gamma^2$ from the target, it is necessary also to take into account corrections to the wave zone approximation, whose effect is, in last instance, in reducing the effective size of the emitting screen.

References

- [1] D.X.Wang, Proc. of 1997 Particle Accelerator Conference , Vancouver, Canada, May 1997, p.1976.
- [2] M.Ferrianis, Proc. of 1998 European Particle Accelerator Conference, Stockholm, Sweden, June 1998, p.159.

- [3] N.F.Shul'ga and S.N.Dobrovol'skii, Pis'ma Zh. Eksp. Teor. Fiz. **65**, 581 (1997) [JETP Lett. **65**, 611 (1997)].
- [4] A.P.Potylitsin, Nucl. Instr. and Methods in Phys. Res., **B145**, 169 (1998) .
- [5] N.F.Shul'ga, S.N.Dobrovol'skii and V.G.Syshchenko, Nucl.Instrum. Meth in Phys. Res., **B145**, 180 (1998) .
- [6] W.Barry, AIP Conference Proceedings 390 (1997) 173; Proc. of the 7th Beam Instrumentation Workshop, Argonne, May 1996.
- [7] R.Lai and A.J. Sievers, Phys.Rev.**E 50**, 3342 (1994).
- [8] A.Murokh, J.B.Rosenzweig, M.Hogan, H.Suk, G.Travich and U.Happek, Nucl. Instr. and Methods in Phys. Res., **A410**, 452 (1998) .
- [9] M.Castellano and V.A Verzilov, Phys. Rev. ST- Accel. Beams, 1, 062801 (1998).
- [10] M.Born and E.Wolf, *Principles of Optics* (Pergamon Press, New York, 1965).